

Empirical and Numerical Evaluation of a Cut Slope Near Rishikesh, India



V. H. R. Pandey, Ashutosh Kainthola, and T. N. Singh

Abstract The stability analysis of cut slopes along any transportation corridor is necessary to safeguard people's and societal interests. The present work presents assessment of a steep rock cut slope near Rishikesh, along a national highway in Uttarakhand, India. The work details empirical and numerical examination of the slope stretching approximately 20 m in length along the road. The field investigation has been undertaken to ascertain discontinuities conditions, their orientations, spacing between them, geological strength index as well as slope geometries. Three joint sets were recorded with spacing of 10–120, 5–45, 6–35 cm respectively, with slope angle of 75° and slope height equal to 65 m. Moreover, the rock samples were taken in laboratory to further discern required geotechnical parameters such as unconfined compressive strength, Young's modulus, and Poisson's ratio etc. The empirical and numerical techniques were applied to examine the slope's health. Q-slope and Slope Mass Rating were the employed empirical method. Besides, the finite element approach was adopted to assess the slope stability numerical. Finally, outcomes of all these scientific assessments were compared with each other and ground reality. The Q-slope values achieved was 1.58 for the concerned slope, while the SMR value was 37. Finite element simulation yielded a safety factor of 1.6 for the dry condition. Furthermore, kinematic analysis of slope shows the possibility of planar and wedge modes of failures. Keeping in view the attained results, the slope should be excavated at an angle of 69° , while also making provisions for drainage of rain water.

Keywords Q-slope · SMR · Finite element method · Kinematic analysis · Slope stability

V. H. R. Pandey · A. Kainthola (✉)
Department of Geology, Banaras Hindu University, Varanasi, India
e-mail: ashutosh.geo@bhu.ac.in

T. N. Singh
Department of Earth Sciences, IIT Bombay, Mumbai, India

1 Introduction

The population increase and fight for habitable space has led people to settle in perilous hilly terrains [1–3]. People also make their way towards hill stations, to refresh and recharge after exhaustion from daily urban life style [4, 5]. India offers plethora of natural, cultural and historical picturesque sites that soothes tired minds and engender mental health. Tourism brings livelihood for locals and boost nation's economy [3]. Therefore, to attract greater number of visitors across the world and cater the needs of inhabitants, government fosters the development of safer infrastructures such as highways, bridges, railways tracks and tunnels [6, 7]. Also, access to high hills is crucial for the national security of India [8–10]. In the recent decades, India has shown a tremendous growth in civil works and extended its transportation network in various parts of the country, including several hilly, coastal and forested regions. This implementation of roadways requires assessment of various risks, before and after constructions [11–13]. Eventually, a rigorous evaluation of geological and geotechnical parameters of slope masses are enforced, and accordingly, construction is being planned [14–16]. The main motive of these slope examinations is to avoid danger of slope failure, rockfall, and debris flow using well planned engineering techniques [17–19].

Workers adopts well-studied assessment methods to check the stability of slopes, according to prevailing geological- geotechnical conditions and need [20]. Transportation of smaller vehicles requires narrower pathways, whereas heavy vehicles demand wider and more stable ones. Hence, agencies plan construction according to work load and time duration, without exploitation of available resources [21, 22]. Engineering geologists and civil engineers work together to achieve fastest, safest, economic and eco-friendly transportation network [23–25]. Geotechnical properties like cohesion, angle of internal friction, Poisson's ratio, Young's modulus, geological strength index (GSI), and UCS etc., form an essential component of stability analysis [26]. Besides, structural discontinuities present in the rock mass affect the slope's health based on their orientation, persistence, spacing, aperture, roughness and alteration [27]. Moreover, slope geometry such as slope height, slope angle, and slope shape have a major say in it. Apart from all these controlling factors of slope failure, several triggering attributes such as rainfall, glacier melting, earthquakes, and ground vibrations (due to heavy vehicles movement, blasting, and other human activities) dominates the occurrence of failure events [3, 28]. Therefore, an advance knowledge of aforementioned attributes can be viable for humankind to deal with landslides and slope failures.

The present work illustrates empirical and numerical assessment of slope, stretching 20 m across the road. The road connects the Rishikesh and Badarinarth, which is a major transportation corridor, supporting tourism and pilgrimage in Garhwal Himalayan region. Through this way, thousands of people enter the valley and further north. People's safety is of major importance for the government agencies, so their employees always have eye on the associated risk and take appropriate actions. The concerned road runs parallel to the river Ganga, which is perennially

flowing. Often, toe erosion of road can become severe, mainly during rainy seasons when river flows in full capacity & high velocity. The area receives significant amount of rainfall in between months of June and September each year, and reports of slope failure and landslide rises across the region.

2 Geological Framework

The geological setup of the study area is quite complex, as it belongs to the Lesser Himalayan terrain (Fig. 1) [29]. The mighty Himalaya originated as a result of tectonic collision between Indian and Eurasian plates in the geologic history [30]. The Indian plate subducted below the Eurasian plate which resulted in a large-scale folding, faulting, fracturing along with several volcanic processes [31]. As one moves northward from the Gangetic plain will pass through Shiwaliks, Lesser Himalaya, Higher Himalaya, and Tethys Himalaya on crossing Main Frontal Thrust (MFT), Main Boundary Fault (MBT), Main Central Thrust (MCT), and Indus Tsang-Po suture zone (ITSZ) respectively [32]. Beside, many other small to medium scale faults can be located in the Himalayan region [33]. The tectonic movements are still at work, which are causing several other new structural disturbances in the area.

The peculiar research area belongs to the Garhwal Himalaya of the Lesser Himalayan region of Uttarakhand. The area suffers from intense rainfall activity, temperature fluctuation, seismicity, and wind action, which are continuously deteriorating the rockmass conditions [29]. Consequently, the hill slopes are susceptible to failure and can lead to a calamity. Stratigraphically, Garhwal Himalaya has been demarcated into Tejam, Ramgarh, Jaunsar, Mussoorie, Damtha, Sirmur, and Almora groups [34]. The study area consists of metasedimentary sequences of rocks

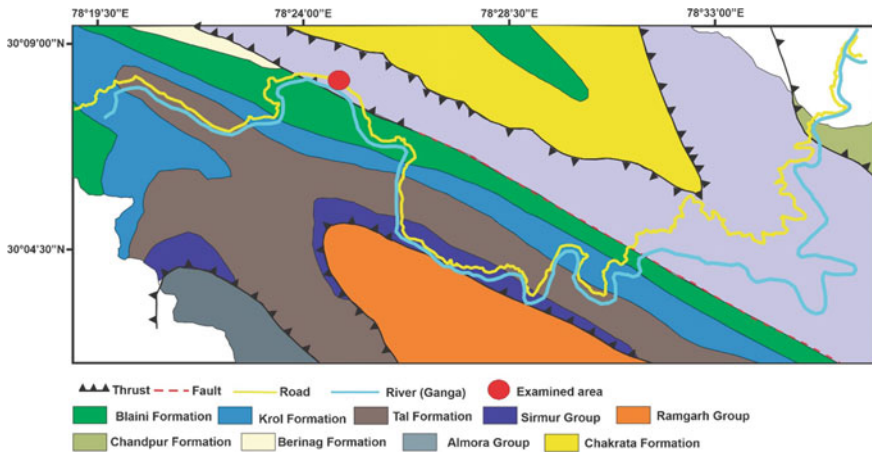


Fig. 1 Geological setup of the examined site (modified after Pradhan and Siddique [29])

belonging to Infra-Krol, Chakrata, Krol, Tal, Nagthat, and Blaini formations [35]. Therefore, shale, siltstone, limestone, sandstone, dolomite, and quartzite dominate the tectonically deformed lithology of the hilly terrains, which are ultimately cut by several perennial and rainfed streams. The studied rock cut-slope have proximity with MBT as well as the Ganga River flows parallel to it on the other side of the highway NH-52.

3 Methodology

The work was commenced with a scrupulous field investigation, followed by certain laboratory testing, afterwards empirical and numerical analysis were carried out. Moreover, based on the analysis results and field conditions the best possible slope scenario is pictured and assessed in the study. To begin the analysis part of the study, initially the kinematic assessment of slope and possible modes of structural instability were identified. The results of the kinematic analysis played a key role in further determination of Q-slope and SMR. Finally, a finite element analysis was carried out to ascertain the factor of safety of slope.

3.1 Kinematic Analysis

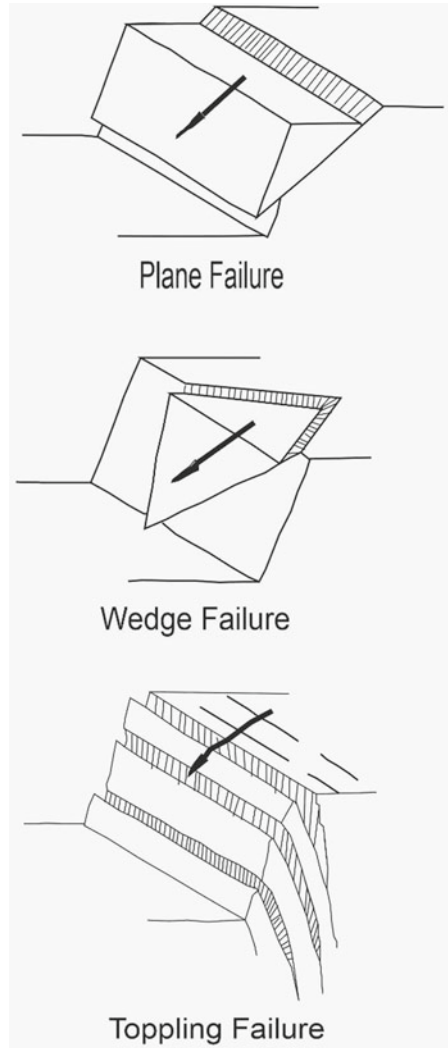
Kinematic analysis of slopes implies examining possible movements owing to rock-mass discontinuities relative to slope orientation, without involving forces [14]. Planar failure, wedge failure, and toppling failure are three modes of instability associated with relationship between geologic structures of bedrock and slope face (Fig. 2) [36]. Furthermore, the kinematic study of cut-slopes does not take cohesion into the consideration. However, the angle of internal friction associated with the joint planes finds application in the study [37].

Chances of plane failure becomes prominent when slope face and any joint plane has a nearly parallel (or within the limits of 20°) dip direction, and the joint should daylight on the slope face. Apart from this, joint should dip steeper than associated angle of internal friction along the joint plane. The conditions of plane failure can be demonstrated mathematically as in the Eqs. (1), if α , β , and γ are slope angle, joint dip, and angle of internal friction along the joint planes respectively [38].

$$\alpha > \beta > \gamma \quad (1)$$

Wedge failure is a play of two intersecting joints, if the line along their intersection plunges lower than the rock-slope angle and higher than the angle of internal friction. In this scenario a wedge of rockmass will slip outward from a rock slope, and can be a source of potential threat to nearby population or travelers depending on their volume. The wedge failure scenarios can be expressed using arithmetic Eqs. 2, if θ

Fig. 2 Modes of slope failure along discontinuities



is the plunge of line formed by intersecting joint planes [37]. Sometimes, it has been observed that wedge can slide along a single plane owing to its favorable conditions for sliding, in comparison to both the planes (or line of their intersection).

$$\alpha > \theta > \gamma \tag{2}$$

Toppling instability are enabled, if the discontinuities dip steeply into the slope face, as well their strikes are nearly parallel (within 30°). This instability scenario can be shown mathematically using Eq. 3 [38]. Workers have addressed two kinds of toppling failure, i.e., flexural toppling and direct toppling.

Table 1 Structural data associated with the rock-mass and slope

Discontinuities	Dip amount	Dip direction
Slope face	75°	240
J ₁	56°	226
J ₂	24°	305
J ₃	80°	120

$$(90 - \beta) + \gamma < \alpha \tag{3}$$

In the present work, three set of joints have been identified in the rockmass and a cut-slope for the development of Rishikesh-Badarinath highway was designed to make timely and safer transportation of goods and services in the region. Table 1 provides major structural set of the cut-slope, and Fig. 3 will illustrate rockmass conditions at the examined site.



Fig. 3 Rockmass conditions of the cut-slope in the study area

3.2 Q-Slope

The technique enhances the workers capability to examine rock cut-slope stability in real time [39]. Once the fresh rock conditions are exposed during excavation, Q-slope enables the engineer to decide the maximum slope angle without any engineered support [40]. The method is empirically derived from Q-system (applied in tunnels), owing to numerous pragmatic observations across the planet. One needs to ascertain six parameters to determine the Q-slope value (Eq. 4), namely, Rock Quality Designation (RQD), Joint set number (J_n), Joint roughness number (J_r), Joint alteration number (J_a), Geological and Environmental condition number (J_{wice}), and strength reduction factors SRF_{slope} [41]. Consequently, the maximum angle at which slope will be stable without implementation of any engineering solution can be enumerated as (Eq. 5) [42].

$$Q_{slope} = \left(\frac{RQD}{J_n} \right) * \left(\frac{J_r}{J_a} \right) * \left(\frac{J_{wice}}{SRF_{slope}} \right) \tag{4}$$

$$\beta_{20} * \log_{10}(Q_{slope}) + 65^\circ \tag{5}$$

RQD of the rockmass depends on the spacings between the available discontinuities, and is simple percentage of intact rock core lengths greater than 10 cm of the total core length (Eq. 6). Beside, another evaluation approach for RQD is to determine the spacing between each joint sets and deploy the Eqs. 7 and 8 [43].

$$RQD = \frac{\sum \text{Length of core pieces} > 0.1m}{\text{Total length of the core run}} * 100\% \tag{6}$$

$$J_v = \frac{1}{S_1} + \frac{1}{S_2} + \frac{1}{S_3} + \dots + \frac{1}{S_n} \tag{7}$$

$$RQD = 115 - 3.3J_v \tag{8}$$

J_n can be estimated by counting the number of joint sets and random joints and then examining the work of Bar and Barton [40]. Similarly, one will be able to decipher the values of J_r , J_a , J_{wice} , and SRF_{slope} with evidences from field setting and available literatures [39–42]. In case of “ J_r/J_a ” an orientation factor is worked out and depending on the kinematic assessment most critical joint set is identified with respect to slope orientation. Moreover, in case of wedge failure both the discontinuity planes are considered in evaluation of “ J_r/J_a ” along with a suitable and separate orientation factor for each of them. The orientation factor can be inferred from the previous works of Q-Slope [40, 44]. Furthermore, SRF_{slope} have three ways to be examined, therefore all the possible ones (SRF_a , SRF_b , and SRF_c) should be analyzed and the one with highest value should be assimilated in the work.

To discern the Q-slope value in the study area, all the six parameters were marked based on the field investigation, climatic condition prevailing at the site, and basic

Table 2 Q-slope attributes pertaining to the study area [40–42]

Parameters	Numeric values	Description
RQD	90–100	Excellent rockmass
J _n	9	Three joint sets are present
J _r	3	Rough or irregular, undulating
J _a	4	Sandy particles, clay free disintegrated rock
J _{wice}	0.5	Stable structure and competent rock lying in tropical storm condition
SRF _{slope}	SRF _a = 2.5; SRF _b = 2.5; SRF _c = N/A (Maximum among these will be adopted in the study)	SRF _a : Slight loosening due to surface location, disturbance from blasting or excavation SRF _b : high stress-strength range SRF _c : not applicable as there are no major discontinuity plane

mathematical assessment, taking reference from available literature. Table 2 highlights all the numeric values of each attribute entrained in the determination of Q-slope belonging to the study area. Therefore, considering Table 2 and Eq. 4, one can evaluate Q-slope value. Eventually, maximum angle at which slope will be stable without implementing any engineering support can be deciphered through Eq. 5.

$$Q_{slope} = \left(\frac{95}{9}\right) * \left(\frac{3}{4}\right) * \left(\frac{0.5}{2.5}\right)$$

$$Q_{slope} = 1.58$$

$$\beta_{20} * \log_{10}(1.58) + 65^\circ$$

$$\beta = 68.97^\circ$$

3.3 Slope Mass Rating

Slope mass rating (SMR) is another method to assess the slope stability conditions, and an exquisite combination of rock mass rating (RMR_{basic}) and certain adjusting factors justifying the modes of failures associated in the cut slope [45, 46]. RMR_{basic} is a summation of certain rock mass parameters such as unconfined compressive strength (UCS), RQD, Joint Spacing, Discontinuity conditions and groundwater situation prevailing at the site (Eq. 9) [47–50]. Moreover, SMR can be enumerated using Eq. 10. The data pertaining to determination of SMR of the examined area can be

Table 3 Rock mass rating (basic) parameters of the study area [46–48]

Parameters	Description	Range of values
UCS	36 MPa	4
RQD	90–100%	20
Spacing	$S_1 = 200\text{--}600$ mm	10
Conditions of discontinuities	Slightly rough surface, Separation < 1 mm, highly weathered walls	20
Groundwater	Completely dry	15

Table 4 Adjustment ratings for joints in case of plane failure [46–49]

Cases	Range	Adjustment factors	Values
$ \alpha_j - \alpha_s = 240^\circ - 226^\circ = 14^\circ$	$20^\circ\text{--}10$	F_1	0.70
$\beta_j = 56^\circ$	$>45^\circ$	F_2	1.00
$(\beta_j - \beta_s) = (56^\circ - 75^\circ) = -19^\circ$	$<-10^\circ$	F_3	-60.00
Slope excavation method	Presplitting	F_4	10.00

where, α_j , α_s , β_j , and β_s are the joint dip direction, slope dip direction, joint dip and slope dip respectively

inferred from Tables 3 and 4.

$$RMR_{basic} = UCS + RQD + S + CD + GW \tag{9}$$

$$SMR = RMR_{basic} + [(F_1 F_2 F_3) + F_4] \tag{10}$$

Calculation of RMR_{basic} will be evaluated using above mentioned Eq. (9).

$$RMR_{basic} = 4 + 20 + 10 + 20 + 15$$

$$RMR_{basic} = 69$$

Hence, the rockmass falls under class number II and considered to be “good rock” [48]. Finally, we needed parameters such F_1 , F_2 , F_3 , and F_4 to estimate the SMR of the rockmass of the study area. So, one will have to establish the discontinuities to discern the probable modes of kinematic stability of the slope being examined.

Now, as per kinematic analysis planar and wedge modes of failures were identified. However, toppling failure is not possible for the given structural set of the rockmass and the slope. Therefore, one will have to enumerate the F_1 , F_2 , F_3 , and F_4 based on the planar failure features [45, 49]. The mathematical analysis presented below will form the base for the further estimation of concerned values.

So, using Eq. (10) SMR can be estimated based on determined RMR_{basic} and other adjusting factors as mentioned in Table 4.

$$SMR = 69 + [(0.70 * 1 * (-60)) + 10]$$

$$SMR = 37$$

3.4 Finite Element Analysis:

The pace of growth in last few decades is attributed to technical advancement in computing technology [51]. Every single sphere of the planet has seen an enormous change with advent of new methods of solving complex mathematical equations, that too with quite greater accuracy and precision in short span of time. The rapid development in new technologies defines several new chapters in various aspects of scientific era. Consequently, the geotechnical domain has witnessed enormous growth in later half of 20th century with introduction of numerical methods [52–54]. These numerical methods are much faster and efficient in deciphering the geomechanical responses than most of the established traditional methods [55]. Numerical simulations are devoid of several assumptions, and all the arithmetic operations are performed in numerous small elements which are connected with each other through nodes [56]. The number of elements and type of nodes adopted in model have significant impetus on time requirement and precision of the results [56, 57]. The physico-mechanical behavior of rockmass and soil material under constant static and dynamic loading can be enumerated with confidence in any underground opening or cut slopes [52]. The numerical techniques have, i.e., continuum, discontinuum, and hybrid modelling [29]. The continuum approach deals with uniform distribution pattern of physical and mechanical attributes throughout the structure [29, 54]. While, the discontinuum plays clear under varying engineering and geological properties within any geotechnical projects. Furthermore, hybrid models address where both the continuum and discontinuum conditions are assimilated together. Finite element, finite difference, and boundary element falls under the continuum numerical techniques [58]. In addition, discrete element method and discrete fracture network are reliable discontinuum numerical approaches meant to simulate heterogenous physico-mechanical engineering designs [59].

Considering the site conditions, following the field investigation and laboratory testing, geotechnical properties with respect to slope attributes were examined in finite element method (FEM). The present work performs slope stability assessment under the environment of RS² tool, a product of RocScience bundle. The FEM method will assess the safety factory of the rock cut-slope considering shearing stresses and shear strength of the material. Moreover, the failure zone develops at the points where shearing stresses dominates the shear strength of the material [52–56]. In the

present numerical assessment, shear strength reduction (SSR) technique is involved. In SSR technique the finite element, iteratively reduces the shearing strength of the material by dividing the cohesion and angle of internal friction with a numerical entity (factor), until the material fails to support the resulting stress acting on the slope (Eqs. 11 and 12) [58–64].

$$c' = \frac{c}{FoS} \tag{11}$$

$$\varphi = \arctan\left(\frac{\tan\varphi}{FoS}\right) \tag{12}$$

On observing the rockmass conditions and taking clues from the past literature, the present study adopts the Generalized Hoek–Brown (GHB) failure criteria for finite element calculations [55–57]. The GHB failure criteria governs the failure mechanisms of the rockmass in a pragmatic manner, developing slip surface either along discontinuities or within the intact rock, and sometimes through both at the same time (Eqs. 13 and 14) [29, 57, 60].

$$\sigma'_1 = \sigma'_3 + \sigma_{ci} \left(m_b \frac{\sigma'_3}{\sigma_{ci}} + s \right)^a \tag{13}$$

$$m_b = m_i * \exp\left[\frac{(GSI - 100)}{28} \right] \tag{14}$$

where, $\sigma'_1, \sigma'_3, \sigma_{ci}$, are the major effective principal stress, minor effective principal stress, uniaxial compressive strength of the intact rock respectively. Besides, m_i is the rock type dependent material constant. Moreover, s and a are based on disturbance factor (D) and GSI curve fitting parameters. Nonetheless, one can evaluate the values of s and a for good quality ($GSI > 25$) rocks using Eqs. (15 and 16) [29] and bad quality ($GSI < 25$) rocks using Eqs. (17 and 18). In the present rockmass determined GSI value is 45–55, which will be used here in finite element calculation, to satisfy the GHB failure criteria requirements.

$$s = \exp[(GSI - 100)/9] \tag{15}$$

$$a = 0.5 \tag{16}$$

$$s = 0 \tag{17}$$

$$a = 0.65 - GSI/200 \tag{18}$$

Therefore, the factor of safety of the rock cut-slope can be established in RS² program, employing FEM over SSR technique and GHB failure mechanism.

4 Results and Discussion

Slope stability examination kinematically discern that there are two possible modes of slope failure. The planar failure is possible along the J1 joint set, which can be a source of major destruction (Fig. 4a). Moreover, the risk of wedge failure is high along the line of intersection of joint sets J₁ and J₃, also a little chance of wedge failure along the line formed by intersection of J1 and J2 (Fig. 4b). Moreover, the study shows that the chances of toppling is quite negligible (Fig. 4c, d).

After the kinematically evaluating the slope sliding, the work further digs into few empirical techniques of slope stability examination. In this row, Q-slope and SMR techniques were analyzed in the study. Moreover, the relevant parameters required in ascertaining the results of these methods were carefully studied during field and laboratory investigations. Furthermore, the assessed parameters were marked numerically apropos to works of earlier researchers. In the present research, the value of Q-slope is 1.58, which means that a slope angle of approximately 69° will be ideally stable without any needed support structure. However, at present state rock cut-slope is standing at an angle of 75° without any support, which is little higher than the estimated value through Q-slope technique. The standing slope is slightly steeper than the calculated one, so a small instability may be rendered owing to extreme conditions like heavy rainfall or high magnitude earthquakes. As, the region is prone to higher duration of rainfall period, it will lead to development of pore water pressure in the fracture or other cracks within the rockmass. Consequently, stable slopes

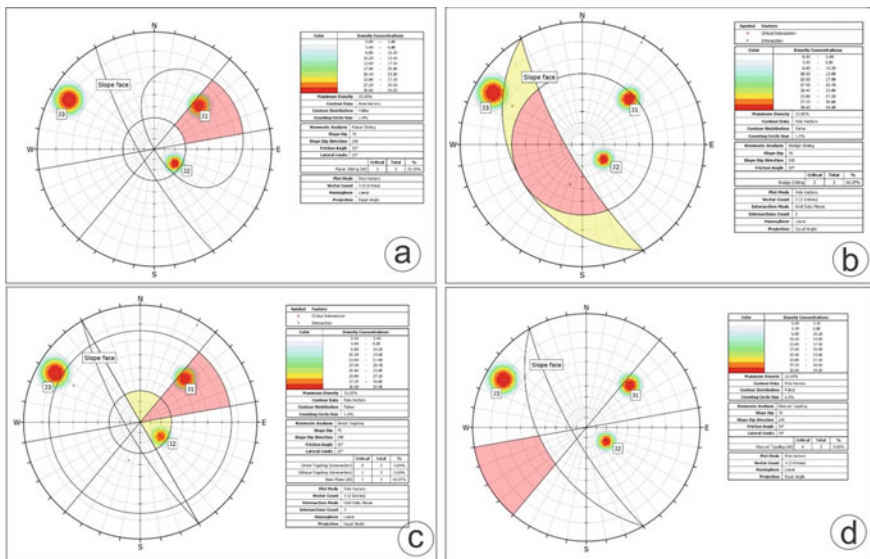


Fig. 4 Pictorial representation of kinematic analysis of the studies slope **a** planar sliding, **b** wedge sliding, **c** direct toppling, **d** flexural toppling

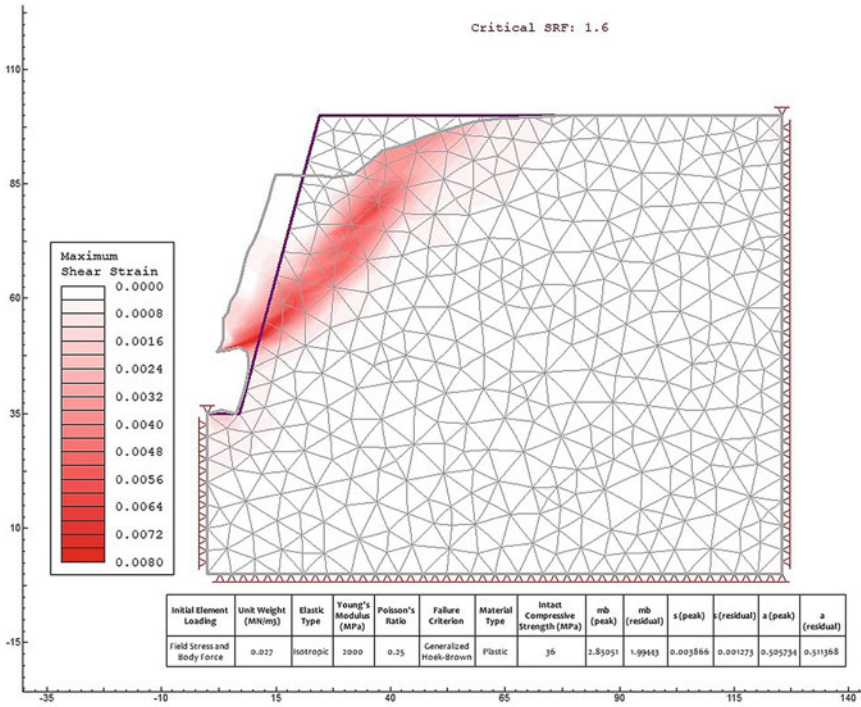


Fig. 5 Finite element analysis of studied rock cut-slope with safety factor and maximum shear stress distribution, moreover showing deformed boundary. Furthermore, scale is in meter with boundary condition suitable for numerical methods

will become precarious and may fails. Similarly, seismic events will exacerbate the shear strength of the intact and rockmass, and will render instability to the rock cut-slopes in the region. However, in hilly terrain of the Lesser Himalaya higher magnitude tremors are rare, so there are quite meagre chances of instability owing to earthquakes in the examined area. In the light of apropos discussion here, author will suggest the authorities to drainage holes in the slopes to avoid any casualty in the future.

The other empirical method employed in the present research, i.e., slope mass rating earns a numerical value of 37. Following, the RMR_{basic} examination in the process of SMR calculation provides an arithmetic number 69. The RMR_{basic} signifies that rockmass can be grouped into class II, a good rock quality based on the previous literatures. The SMR evaluation will need adjusting factors to be summed into the RMR_{basic} numerical value. Also, based on the kinematic study of slope stability, the most probable mode of failure was planar type. Hence, taking the outcomes of

kinematic analysis and other slope and discontinuities relationships the adjustment factors were enumerated in the study. Moreover, F_1 , F_2 , F_3 , and F_4 are 0.70, 1.00, –60.00, and 10 respectively. Additionally, the SMR value lies at the border of bad and normal quality rockmass, it can be concluded that slope stability will vary from being unstable to partially stable one. Therefore, support is necessary to make cut-slope safer for people.

On the other hand, the numerical stability assessment in finite element tool declares the slope to be stable with a quite higher safety factor. The slope was analyzed in the RS² program with shear strength reduction technique and under the condition of GHB failure criteria. To avoid the complexities the joint conditions were excluded in the FEM examination. The factor of safety for the examined rock cut-slope was 1.6 (Fig. 5).

Based on the techniques like Q-slope and finite element method the slope is stable and does not require any engineering support. However, the slope mass rating declares the slope to be precarious owing to which installation of supports becomes the necessity.

5 Conclusion

The present work is being performed to check the health of a rock cut-slope, which spread almost 20 m in length along the national highway-52. The study area is located in the Lesser Himalayan zone of the Garhwal region and quite close to MBT. The structural discontinuities developed in the geological past are the ramification of tectonic forces due to collision of Indian and Eurasian plates. These discontinuities are the planes of weakness associate in the rockmass, rendering precarious rock cut-slopes in the mountainous ranges. Moreover, the adverse climatic condition and regular seismicity in the valley are another factor affecting the slope health. Kinematic assessment resulted in the probability of plane failure; however, chances of wedge sliding cannot be neglected here.

The resulting Q-slope values signifies that slope will be stable at an angle of 69°, approximately 6° less than the actual one. According to workers, the slope should be stable without any heavy engineering support installation, however, looking at the other environmental factors drainage pipes needed. Furthermore, the SMR study declares the slope to be unstable, with a small value of 39. Therefore, on the basis of SMR cut-slope requires some engineering solution to deter any future fatalities the region and make the transportation route safer. In fact, change in the blasting method can increase or decrease the SMR value. Hence, the concerned authorities should choose a suitable excavation or blasting approach, that does not harm the strength of the rockmass any further. Additionally, factor of safety (1.6) resulted in the finite element examination is quite favorable in terms of safety of passengers of NH-52.

References

1. Ansari T, Kainthola A, Singh KH, Singh TN, Sazid M (2021) Geotechnical and micro-structural characteristics of phyllite derived soil; implications for slope stability, Lesser Himalaya, Uttarakhand, India. *Catena* 196:104906. <https://doi.org/10.1016/j.catena.2020.104906>
2. Bharati AK, Ray A, Khandelwal M, Rai R, Jaiswal A (2021) Stability evaluation of dump slope using artificial neural network and multiple regression. *Eng Comput* 9:1–9. <https://doi.org/10.1007/s00366-021-01358-y>
3. Kainthola A, Sharma V, Pandey VH, Jayal T, Singh M, Srivastav A, Singh PK, Champati Ray PK, Singh TN (2021) Hill slope stability examination along Lower Tons valley, Garhwal Himalayas, India. *Geom Nat Haz Risk* 12(1):900–921. <https://doi.org/10.1080/19475705.2021.1906758>
4. Ahour M, Hataf N, Azar E (2020) A mathematical model based on artificial neural networks to predict the stability of rock slopes using the generalized Hoek-Brown failure criterion. *Geotech Geol Eng* 38(1):587–604. <https://doi.org/10.1007/s10706-019-01049-y>
5. Daftariresheli A, Ataei M, Sereshki F (2011) Assessment of rock slope stability using the Fuzzy Slope Mass Rating (FSMR) system. *Appl Soft Comput* 11(8):4465–4473. <https://doi.org/10.1016/j.asoc.2011.08.032>
6. Kainthola A, Singh PK, Singh TN (2015) Stability investigation of road cut slope in basaltic rockmass, Mahabaleshwar, India. *Geosci Front* 6(6):837–845. <https://doi.org/10.1016/j.gsf.2014.03.002>
7. Kainthola A, Singh PK, Wasnik AB, Singh TN (2012) Distinct element modelling of Mahabaleshwar road cut hill slope. <http://www.scrip.org/journal/PaperInformation.aspx?PaperID=24023>
8. Khandelwal M, Rai R, Shrivastava BK (2015) Evaluation of dump slope stability of a coal mine using artificial neural network. *Geomech Geophys Geo-energy Geo-resources* 1(3):69–77. <https://doi.org/10.1007/s40948-015-0009-8>
9. Kundu J, Sarkar K, Jaboyedoff M, Singh TN (2019) GISMR: a computer application to perform kinematic analysis, slope mass rating and optimization of slope angle on a GIS platform with the aid of ArcGIS or QGIS. In: AGU fall meeting abstracts, December 2019, vol 2019, pp NH53A-05. <https://ui.adsabs.harvard.edu/#abs/2019AGUFMNH53A..05K/abstract>
10. Kundu J, Sarkar K, Singh AK (2019) EasySMR: a computer program to check kinematic feasibility and calculate Slope Mass Rating. In: Geophysical research abstracts, 1 January 2019, vol 21
11. Mahanta B, Singh HO, Singh PK, Kainthola A, Singh TN (2016) Stability analysis of potential failure zones along NH-305, India. *Nat Haz* 83(3):1341–1357. <https://doi.org/10.1007/s11069-016-2396-8>
12. Rai R, Khandelwal M, Jaiswal A (2012) Application of geogrids in waste dump stability: a numerical modeling approach. *Environ Earth Sci* 66(5):1459–1465. <https://doi.org/10.1007/s12665-011-1385-1>
13. Sardana S, Sharma P, Verma AK, Singh TN (2020) A case study on the rockfall assessment and stability analysis along Lengpui-Aizawl highway, Mizoram, India. *Arab J Geosci* 13(24):1–2. <https://doi.org/10.1007/s12517-020-06196-8>
14. RK U, Singh R, Ahmad M, TN S (2011) Stability analysis of cut slopes using continuous slope mass rating and kinematic analysis in Rudraprayag district, Uttarakhand. *Geomaterials*. <http://www.scrip.org/journal/PaperInformation.aspx?PaperID=8176>
15. Kainthola A, Verma D, Gupte SS, Singh TN (2011) A coal mine dump stability analysis—a case study. *Geomaterials* 1(01):1
16. Kainthola A, Verma D, Thareja R, Singh TN (2013) A review on numerical slope stability analysis. *Int J Sci Eng Technol Res (IJSETR)* 2(6):1315–1320
17. Kundu J, Sarkar K, Singh PK, Singh TN (2018) Deterministic and probabilistic stability analysis of soil slope—a case study. *J Geol Soc India* 91(4):418–424. <https://doi.org/10.1007/s12594-018-0874-1>

18. Kundu J, Sarkar K, Singh TN (2017) Static and dynamic analysis of rock slope—a case study. In: ISRM European rock mechanics symposium-EUROCK. OnePetro
19. Sarkar S, Pandit K, Dahiya N, Chandna P (2021) Quantified landslide hazard assessment based on finite element slope stability analysis for Uttarkashi-Gangnani Highway in Indian Himalayas. *Nat Haz* 106(3):1895–1914. <https://doi.org/10.1007/s11069-021-04518-x>
20. Tiwari VN, Pandey VHR, Kainthola A, Singh PK, Singh KH, Singh TN (2020) Assessment of Karmi Landslide Zone, Bageshwar, Uttarakhand, India. *J Geol Soc India* 96(4):385–393. <https://doi.org/10.1007/s12594-020-1567-0>
21. Rojat F, Labiouse V, Mestat P (2015) Improved analytical solutions for the response of underground excavations in rock masses satisfying the generalized Hoek-Brown failure criterion. *Int J Rock Mech Mining Sci* 79:193–204. <https://doi.org/10.1016/j.ijrmm.2015.08.002>
22. Ray A, Kumar V, Kumar A, Rai R, Khandelwal M, Singh TN (2020) Stability prediction of Himalayan residual soil slope using artificial neural network. *Nat Haz* 103(3):3523–3540. <https://doi.org/10.1007/s11069-020-04141-2>
23. Singh J, Verma AK, Banka H (2018) Application of biogeography based optimization to locate critical slip surface in slope stability evaluation. In: 2018 4th international conference on recent advances in information technology (RAIT). IEEE, pp 1–5. <https://doi.org/10.1109/RAIT.2018.8389070>
24. Singh AK, Kundu J, Sarkar K (2018) Stability analysis of a recurring soil slope failure along NH-5, Himachal Himalaya, India. *Nat Haz* 90(2):863–885. <https://doi.org/10.1007/s11069-017-3076-z>
25. Sharma P, Verma AK, Negi A, Jha MK, Gautam P (2018) Stability assessment of jointed rock slope with different crack infillings under various thermomechanical loadings. *Arab J Geosci* 11(15):1–6. <https://doi.org/10.1007/s12517-018-3772-3>
26. Verma D, Kainthola A, Gupte SS, Singh TN (2013) A finite element approach of stability analysis of internal dump slope in Wardha valley coal field, India, Maharashtra. *Am J Mining Metall* 1(1):1–6
27. Verma D, Thareja R, Kainthola A, Singh TN (2011) Evaluation of open pit mine slope stability analysis. *Int J Earth Sci Eng* 4(4):590–600
28. Wallace CS, Schaefer LN, Villeneuve MC (2021) Material properties and triggering mechanisms of an andesitic lava dome collapse at Shiveluch Volcano, Kamchatka, Russia, revealed using the finite element method. *Rock Mech Rock Eng* 1:1–8. <https://doi.org/10.1007/s00603-021-02513-z>
29. Pradhan SP, Siddique T (2020) Stability assessment of landslide-prone road cut rock slopes in Himalayan terrain: a finite element method based approach. *J Rock Mech Geotech Eng* 12(1):59–73. <https://doi.org/10.1016/j.jrmge.2018.12.018>
30. Yin A (2006) Cenozoic tectonic evolution of the Himalayan orogen as constrained by along-strike variation of structural geometry, exhumation history, and foreland sedimentation. *Earth-Sci Rev* 76(1–2):1–31. <https://doi.org/10.1016/j.earscirev.2005.05.004>
31. Kumar D, Thakur M, Dubey CS, Shukla DP (2017) Landslide susceptibility mapping & prediction using support vector machine for Mandakini River Basin, Garhwal Himalaya, India. *Geomorphology* 295:115–125. <https://doi.org/10.1016/j.geomorph.2017.06.013>
32. Srivastava P, Mitra G (1994) Thrust geometries and deep structure of the outer and lesser Himalaya, Kumaon and Garhwal (India): Implications for evolution of the Himalayan fold-and-thrust belt. *Tectonics* 13(1):89–109. <https://doi.org/10.1029/93TC01130>
33. Bose N, Mukherjee S (2019) Field documentation and genesis of the back-structures from the Garhwal Lesser Himalaya, Uttarakhand, India. *Geol Soc Lond Spec Publ* 481(1):111–125. <https://doi.org/10.1144/SP481-2018-81>
34. Valdiya KS (1980) Geology of Kumaun Lesser Himalaya. Wadia Institute of Himalayan Geology
35. Jiang G, Sohl LE, Christie-Blick N (2003) Neoproterozoic stratigraphic comparison of the Lesser Himalaya (India) and Yangtze block (south China): paleogeographic implications. *Geology* 31(10):917–920. <https://doi.org/10.1130/G19790.1>

36. Zavodni ZM, Broadbent CD (1978) Slope failure kinematics. In: 19th US symposium on rock mechanics (USRMS), 1 May 1978. OnePetro
37. Xiao S, Gao YT, Wu SC, Liu B, Tian QM (2018) Kinematic analysis of slope failure modes based on stereographic projection. In: Progress in civil, architectural and hydraulic engineering IV: proceedings of the 2015 4th international conference on civil, architectural and hydraulic engineering (ICCAHE 2015), Guangzhou, China, 20–21 June 2015. CRC Press, p 313
38. Admassu Y (2013) Shakoor A (2013) DIPANALYST: A computer program for quantitative kinematic analysis of rock slope failures. *Comput Geosci* 1(54):196–202. <https://doi.org/10.1016/j.cageo.2012.11.018>
39. Azarafza M, Nanehkaran YA, Rajabion L, Akgün H, Rahnamarad J, Derakhshani R, Raof A (2020) Application of the modified Q-slope classification system for sedimentary rock slope stability assessment in Iran. *Eng Geol* 264:105349. <https://doi.org/10.1016/j.enggeo.2019.105349>
40. Bar N, Barton N (2017) The Q-slope method for rock slope engineering. *Rock Mech Rock Eng* 50(12):3307–3322. <https://doi.org/10.1007/s00603-017-1305-0>
41. Bar N, Barton NR (2016) Empirical slope design for hard and soft rocks using Q-slope. In: 50th US rock mechanics/geomechanics symposium, 26 June 2016. OnePetro
42. Barton N, Bar N (2015) Introducing the Q-slope method and its intended use within civil and mining engineering projects. In: ISRM regional symposium-EUROCK. OnePetro
43. Palmstrom A (2005) Measurements of and correlations between block size and rock quality designation (RQD). *Tunn Undergr Space Technol* 20(4):362–377. <https://doi.org/10.1016/j.tust.2005.01.005>
44. Song Y, Xue H, Meng X (2019) Evaluation method of slope stability based on the Q slope system and BQ method. *Bull Eng Geol Environ* 78(7):4865–4873. <https://doi.org/10.1007/s10064-019-01459-5>
45. Zheng J, Zhao Y, Lü Q, Deng J, Pan X, Li Y (2016) A discussion on the adjustment parameters of the slope mass rating (SMR) system for rock slopes. *Eng Geol* 17(206):42–49. <https://doi.org/10.1016/j.enggeo.2016.03.007>
46. Tomas R, Cuenca A, Cano M, García-Barba J (2012) A graphical approach for slope mass rating (SMR). *Eng Geol* 124:67–76. <https://doi.org/10.1016/j.enggeo.2011.10.004>
47. Azarafza M, Akgün H, Asghari-Kaljahi E (2017) Assessment of rock slope stability by slope mass rating (SMR): a case study for the gas flare site in Assalouyeh, South of Iran. *Geomech Eng* 13(4):571–584. <https://doi.org/10.12989/gae.2017.13.4.571>
48. Riquelme AJ, Tomás R, Abellán A (2016) Characterization of rock slopes through slope mass rating using 3D point clouds. *Int J Rock Mech Mining Sci* 84:165–176. <https://doi.org/10.1016/j.ijrmmms.2015.12.008>
49. Romana M, Tomás R, Serón JB (2015) Slope Mass Rating (SMR) geomechanics classification: thirty years review. In: 13th ISRM international congress of rock mechanics, 10 May 2015. OnePetro
50. Romana MR (1993) A geomechanical classification for slopes: slope mass rating. In: Rock testing and site characterization. Pergamon, 1 January 1993
51. Chen GH, Zou JF, Zhang R (2021) Stability analysis of rock slopes using strength reduction adaptive finite element limit analysis. *Struct Eng Mech* 79(4):487–98. <https://doi.org/10.12989/sem.2021.79.4.487>
52. Chihi O, Saada Z (2020) Bearing capacity of strip footing on rock under inclined and eccentric load using the generalized Hoek-Brown criterion. *Eur J Environ Civil Eng* 4:1–5. <https://doi.org/10.1080/19648189.2020.1757513>
53. Dyson AP (2018) Tolooiyan A (2018) Optimisation of strength reduction finite element method codes for slope stability analysis. *Innov Infrastruct Sol* 3(1):1–2. <https://doi.org/10.1007/s41062-018-0148-1>
54. Dyson AP, Tolooiyan A (2019) Prediction and classification for finite element slope stability analysis by random field comparison. *Comput Geotech* 109:117–129. <https://doi.org/10.1016/j.compgeo.2019.01.026>

55. Hammah RE, Yacoub TE, Corkum BC, Curran JH (2005) The shear strength reduction method for the generalized Hoek-Brown criterion. In: Alaska Rocks 2005, the 40th US symposium on rock mechanics (USRMS). OnePetro
56. Kumar V, Burman A, Himanshu N, Gordan B (2021) Rock slope stability charts based on limit equilibrium method incorporating Generalized Hoek-Brown strength criterion for static and seismic conditions. *Environ Earth Sci* 80(6):1–20. <https://doi.org/10.1007/s12665-021-09498-6>
57. Lee YK, Pietruszczak S (2021) Limit equilibrium analysis incorporating the generalized Hoek-Brown criterion. *Rock Mech Rock Eng* 5:1–2. <https://doi.org/10.1007/s00603-021-02518-8>
58. Poklopová T, Pavelcová V, Šejnoha M (2021) Comparing the Hoek-Brown and Mohr-Coulomb failure criteria in FEM analysis. *Acta Polytechnica CTU Proc* 30:69–75. <https://doi.org/10.14311/APP.2021.30.0069>
59. Singh J, Banka H, Verma AK (2019) A BBO-based algorithm for slope stability analysis by locating critical failure surface. *Neural Comput Appl* 31(10):6401–6418. <https://doi.org/10.1007/s00521-018-3418-0>
60. Singh J, Banka H, Verma AK (2018) Analysis of slope stability and detection of critical failure surface using gravitational search algorithm. In: 2018 4th international conference on recent advances in information technology (RAIT), 15 March 2018. IEEE, pp 1–6. <https://doi.org/10.1109/RAIT.2018.8389049>
61. Yang Y, Xia Y, Zheng H, Liu Z (2021) Investigation of rock slope stability using a 3D nonlinear strength-reduction numerical manifold method. *Eng Geol* 292:106285. <https://doi.org/10.1016/j.enggeo.2021.106285>
62. You G, Al Mandalawi M, Soliman A, Dowling K, Dahlhaus P (2017) Finite element analysis of rock slope stability using shear strength reduction method. In: International congress and exhibition “sustainable civil infrastructures: innovative infrastructure geotechnology”, 2 July 2017. Springer, Cham, pp 227–235. https://doi.org/10.1007/978-3-319-61902-6_18
63. Zheng H, Liu DF, Li CG (2005) Slope stability analysis based on elasto-plastic finite element method. *Int J Numer Meth Eng* 64(14):1871–1888. <https://doi.org/10.1002/nme.1406>
64. Srivastav A, Pandey VH, Kainthola A, Singh PK, Dangwal V, Singh TN (2021) Numerical analysis of a collapsed tunnel: a case study from NW Himalaya, India. *Indian Geotech J* 1:1–3. <https://doi.org/10.1007/s40098-021-00567-y>